Electronic Supplementary Material (ESI) for Green Chemistry

Supplementary Information

Efficient microalgae harvesting by organo-building blocks of nanoclays†

Wasif Farooq, [a] Young-Chul Lee,*[b] Jong-In Han,[b] Cornelius Hanung Darpito,[a] Minkee Choi[a] and Ji-Won Yang*[a]

[a] Advanced Biomass R & D Center, KAIST, 291 Daehakno, Yuseong-gu, Daejeon 305-701, Republic of Korea. Fax: +82-42-350-3924; Tel: +82-42-350-3910; E-mail: jwyang@kaist.ac.kr

[b] Department of Civil and Environmental Engineering (BK21 program), KAIST, 291 Daehakno, Yuseong-gu, Daejeon 305-701, Republic of Korea. Fax: +82-42-350-3698; Tel: +82-42-350-3610; E-mail: dreamdbs@kaist.ac.kr

Table S1. Parameter values of second order kinetics.

Mg-APTES clay concentration(mg/L)	Second order rate constant(K)	r^2 value
0.25	0.0085	0.712
0.5	0.0173	0.767
1.0	0.0904	0.982

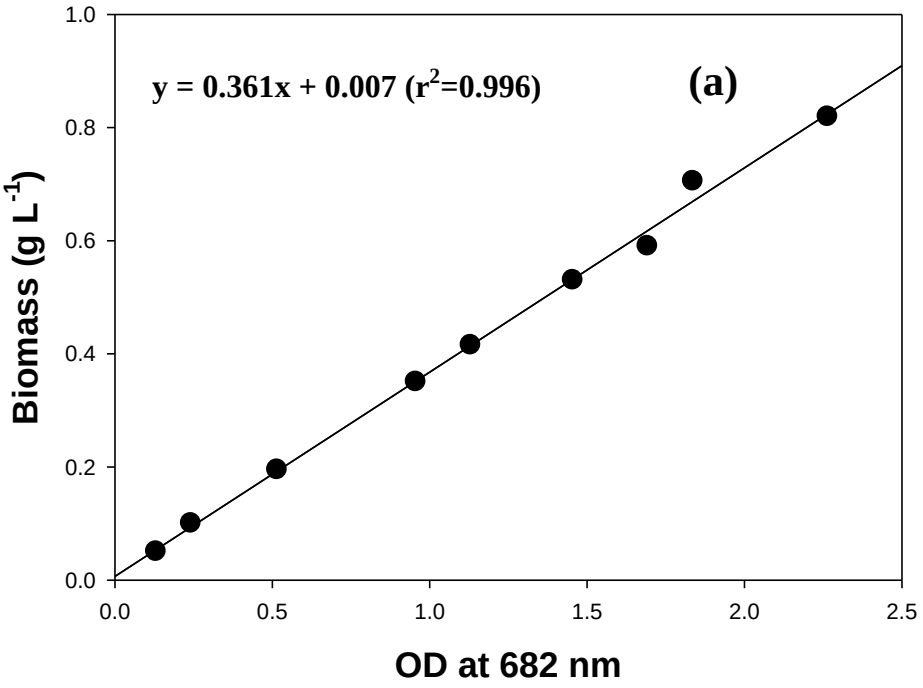

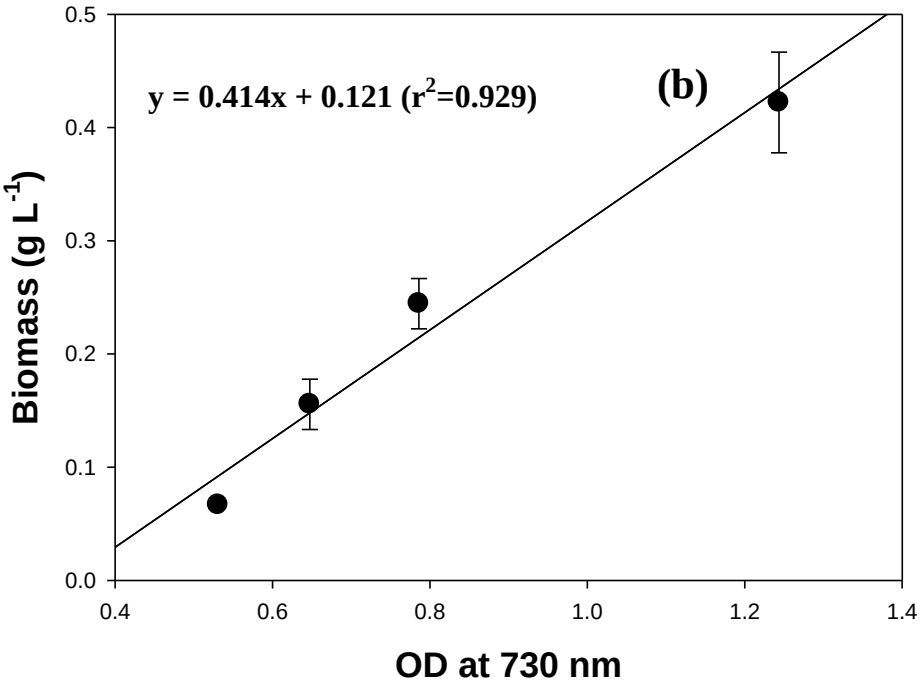

Figure S1. The relationship between OD values and dry biomass (g L^{-1}) where *Chlorella vulgaris* (a) and *Synechocystis* sp. (b), respectively.

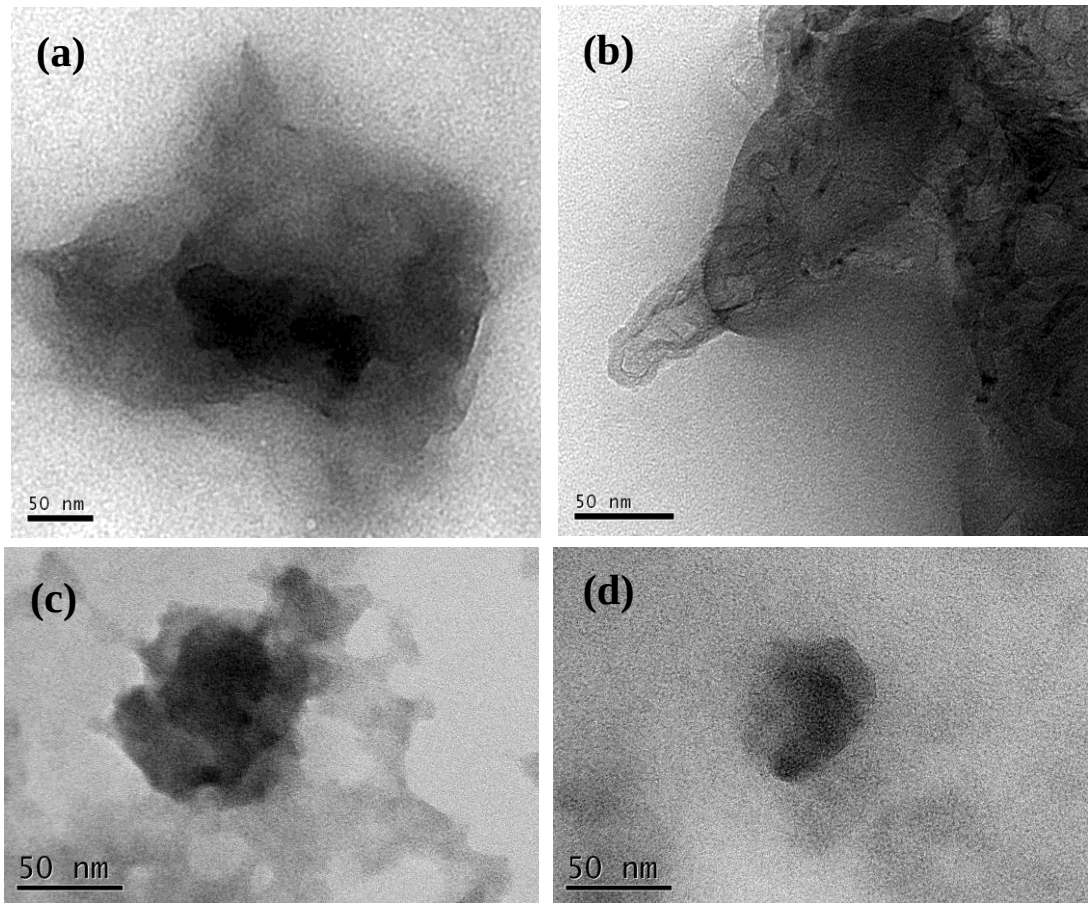

Figure S2. TEM micrographs of Mg-APTES clay (a,b) and Fe-APTES clay (c,d) dispersed in deionized water (0.5 mg mL^{-1}).

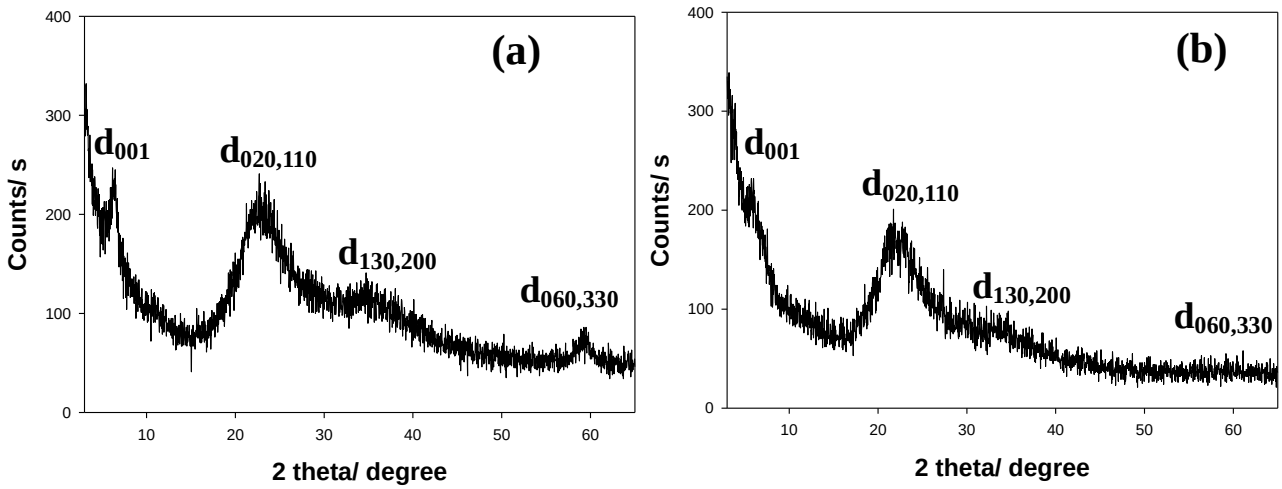

Figure S3. Powder X-ray diffraction (XRD) patterns of Mg-APTES clay (a) and Fe-APTES clay (b).

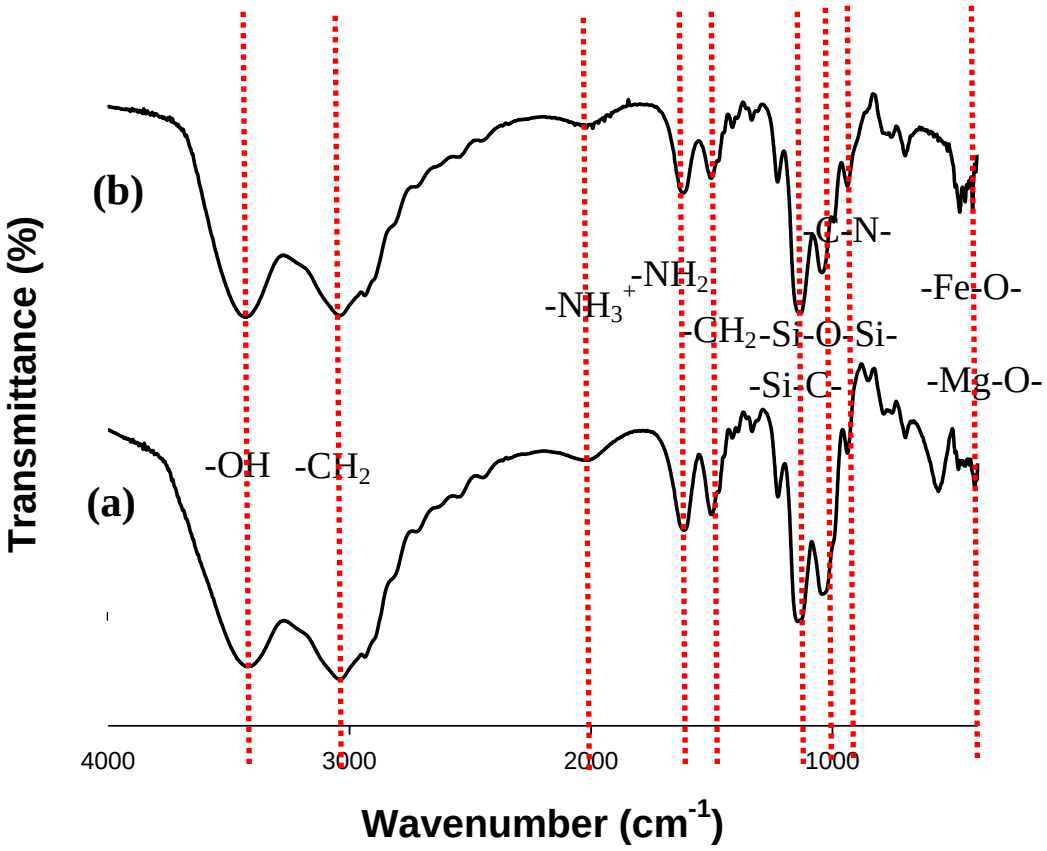

Figure S4. Fourier transform infrared (FT-IR) spectra of Mg-APTES clay (a) and Fe-APTES clay (b).

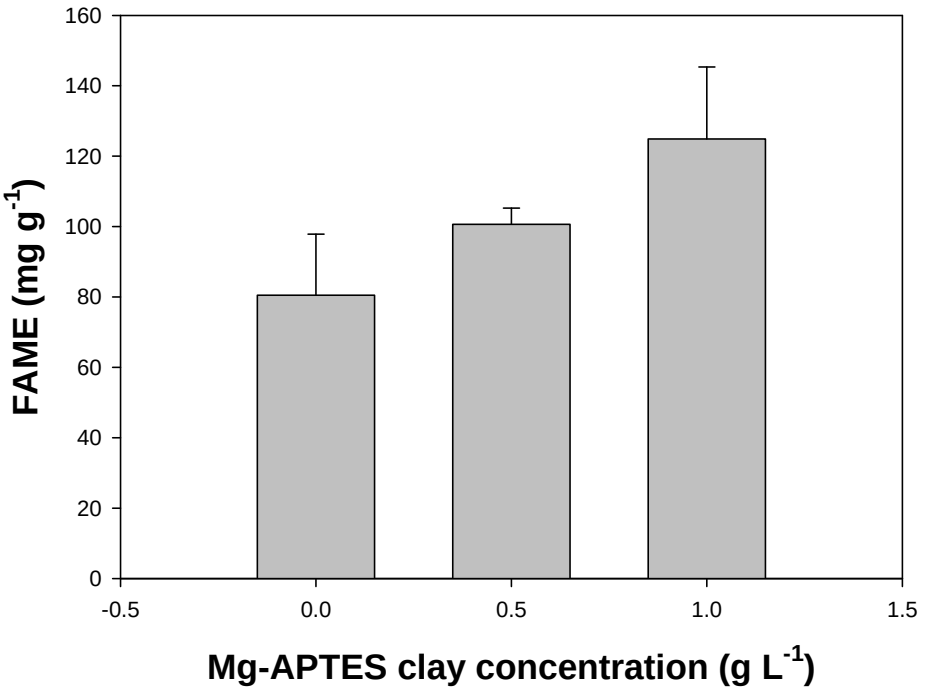

Figure S5. Effect of Mg-APTES clay concentration on fatty acid methyl ester (FAME) of *Chlorella vulgaris*.

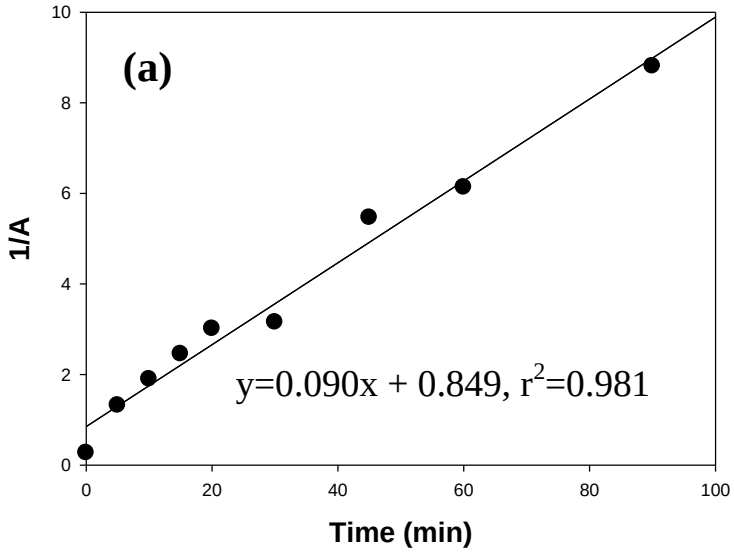

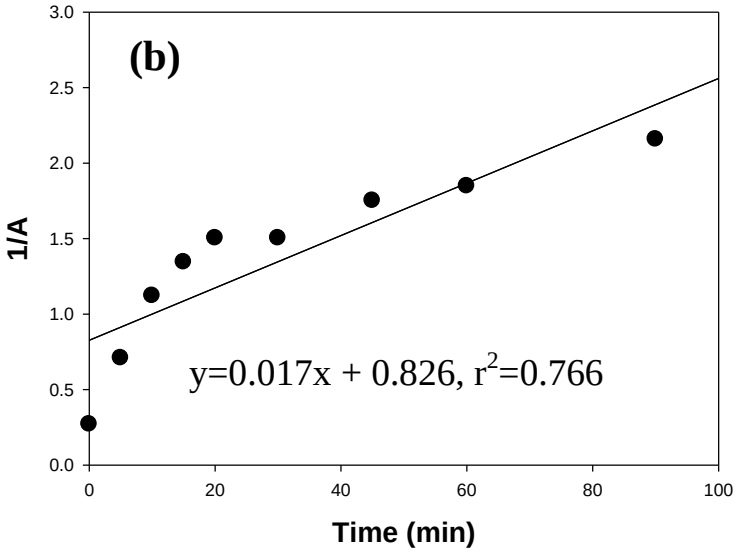

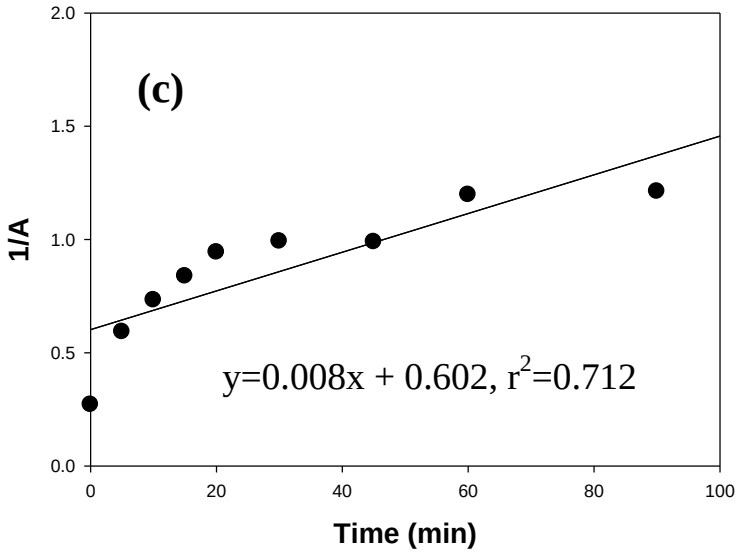

Figure S6. The kinetic plots of microalgae harvesting by 1.0 g/L (a), 0.5 g/L (b), and 0.25 g/L (c) of Mg-APTES clay where the equation was followed, $1/A=kt+1/A_0$ as second order model. Note that A and A_0 is optical density (OD) value at time=t and 0, respectively, and k is rate constant.

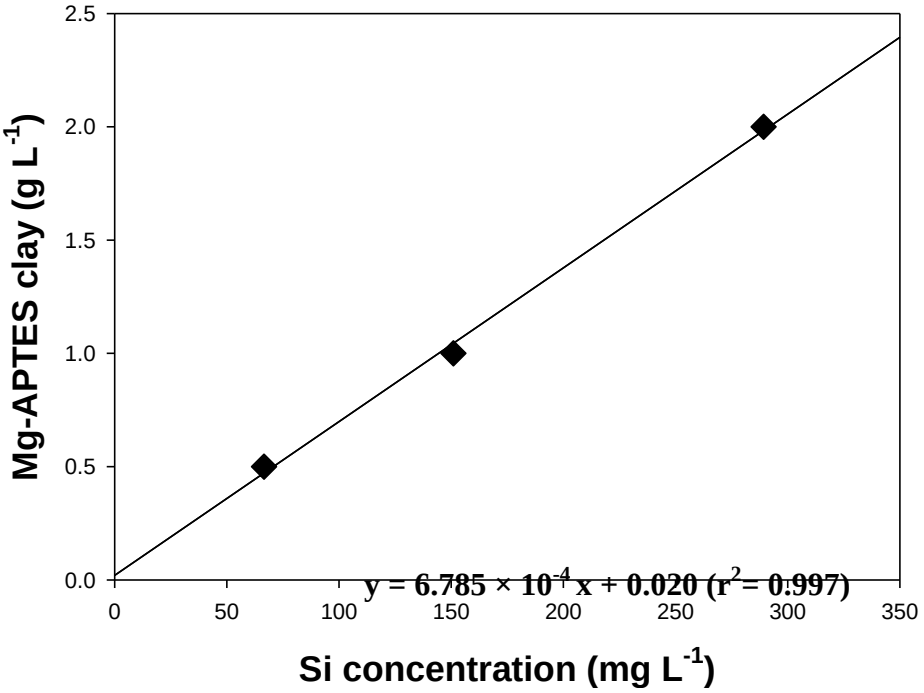

Figure S7. The calibration curve (relationship) of Mg-APTES clay (g L^{-1}) and Si concentration (mg L^{-1}).

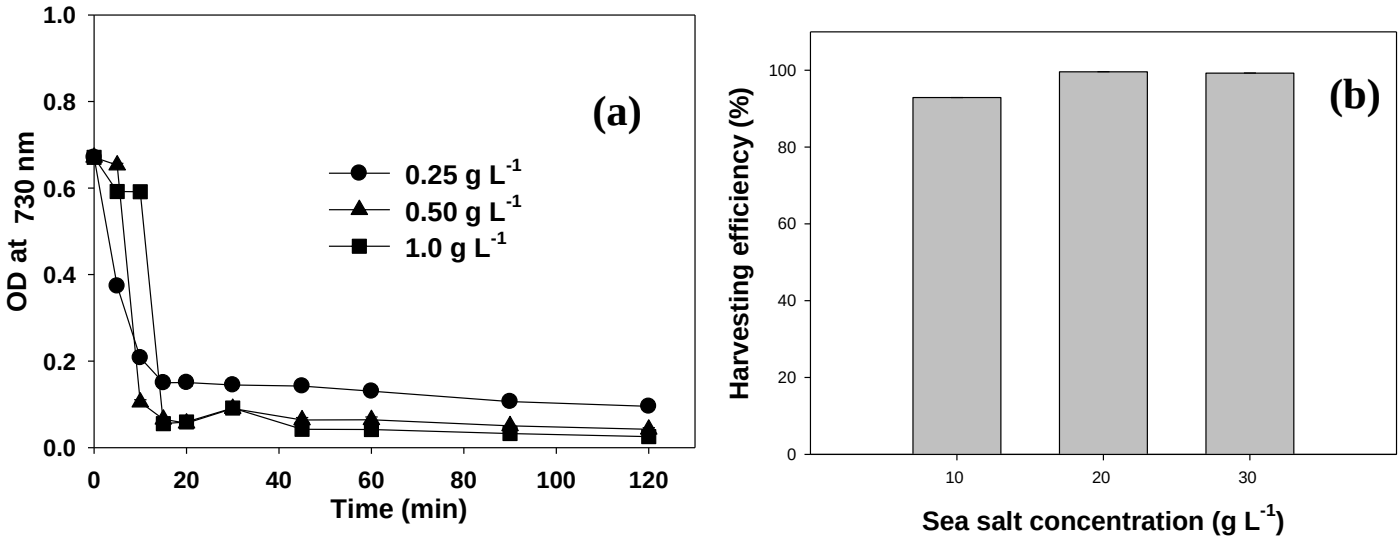

Figure S8. (a) Harvesting of *Synechocystis* sp. by Mg-APTES clay at 1.0 g L^{-1} of microalgae feedstocks and harvesting efficiency (%) (b) of microalga, *Nannochloris oculata* by 1.0 g L^{-1} of Mg-APTES clay at 1.0 g L^{-1} of microalgae feedstocks according to sea salt concentration.

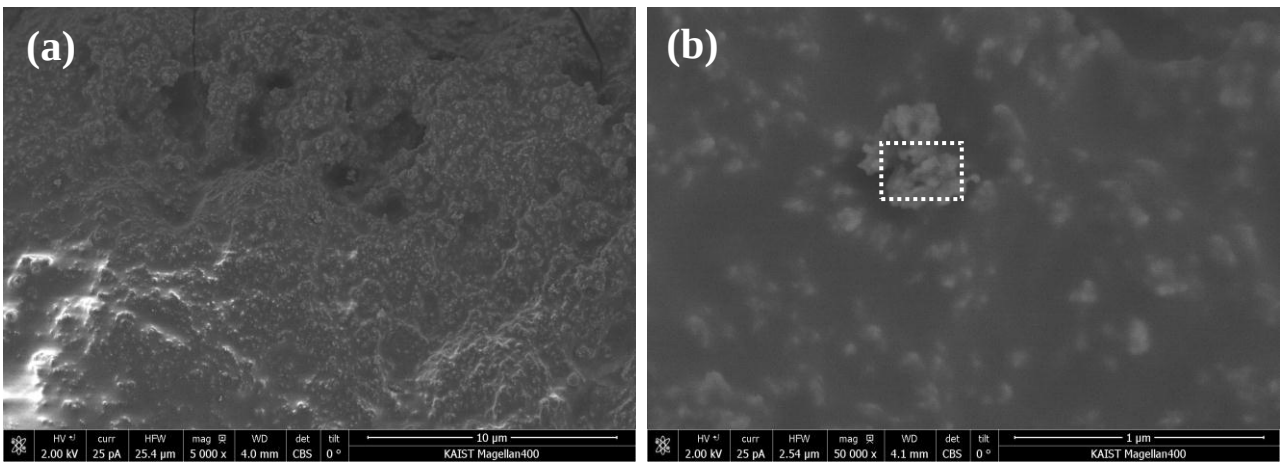

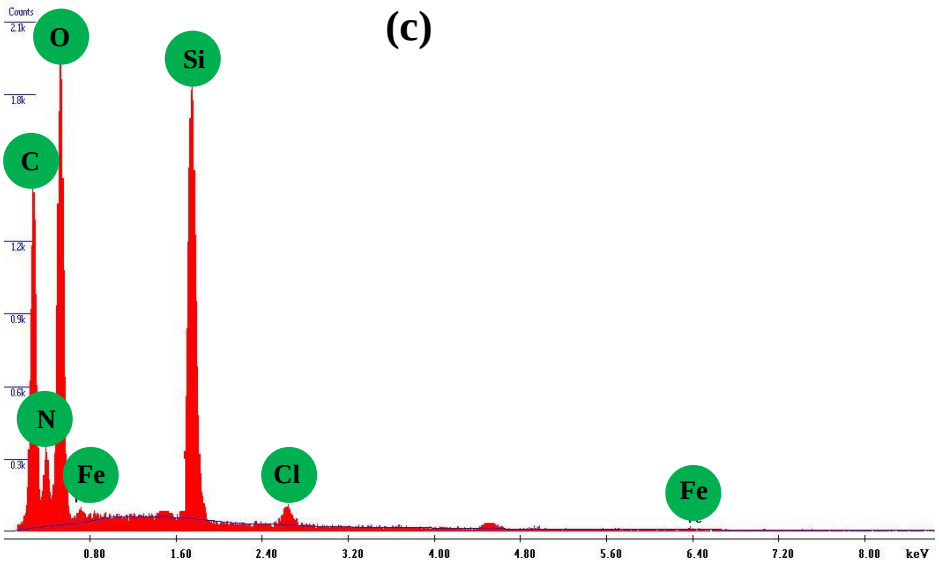

Figure S9. Low magnification image (a) and magnified image (b) of scanning electron microscopy (SEM) micrographs with energy dispersive X-ray microanalysis (EDX, c) for defected Fe-APTES clay-coated onto cotton. Note that the white-dotted rectangular box in (b) indicates the measurement region of EDX analysis.

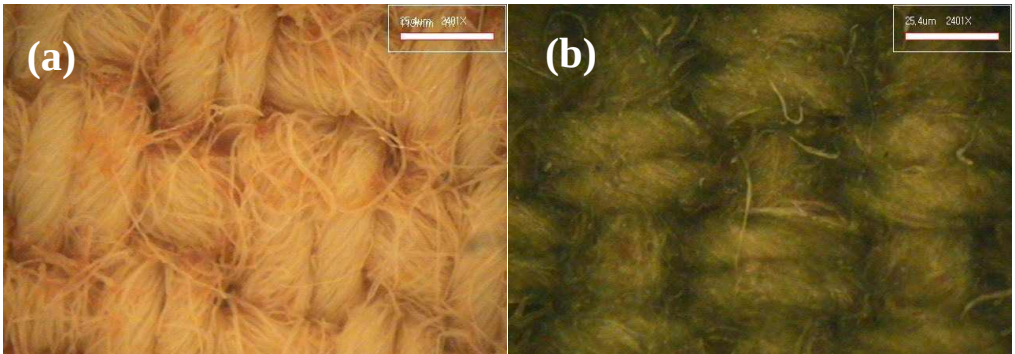

Figure S10. Videoscopic images of defected Fe-APTES clay-coated cotton membrane (runs=2) (a), after microalgae harvesting by defected Fe-APTES clay-coated cotton membrane (runs=2) (b), defected Fe-APTES clay-coated nylon membrane (runs=2) (c), and after microalgae harvesting by defected Fe-APTES clay-coated nylon membrane (runs=2) (d).

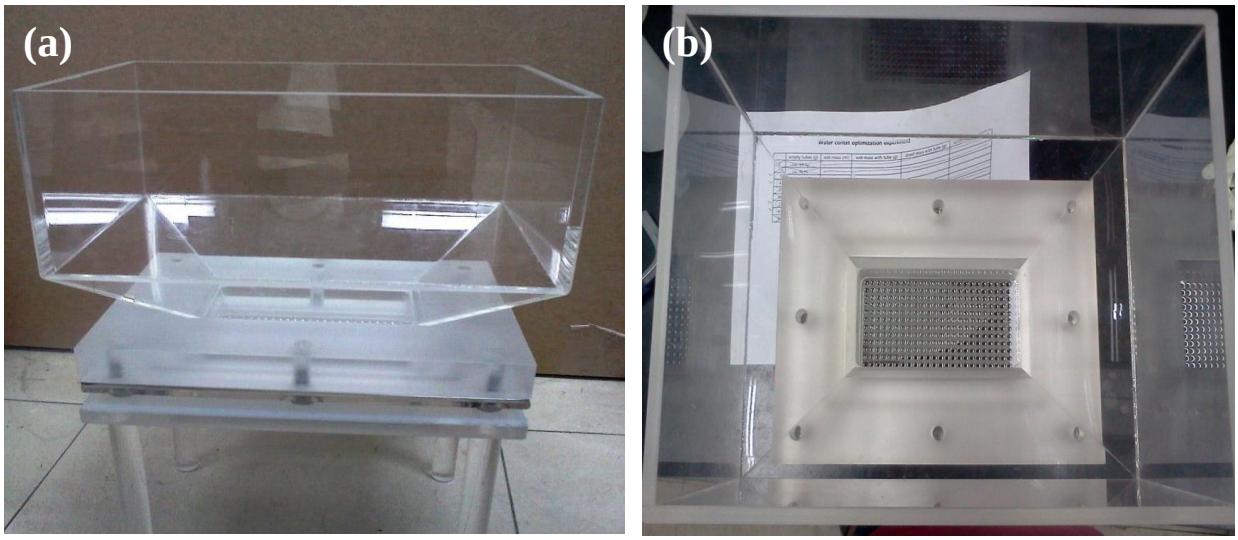

Figure S11. Photographs of front view (a) and top view (b) for filtration equipment (1 L scale) to harvest microalgae biomass.

(b)

(d)

Figure S12. Photographs of microalgae deposited on cotton membrane (a) after harvesting process, its back side (b), collected microalgae biomass on the aluminum foil (c), and after removing microalgae biomass (d) whose cotton membrane was recycled.

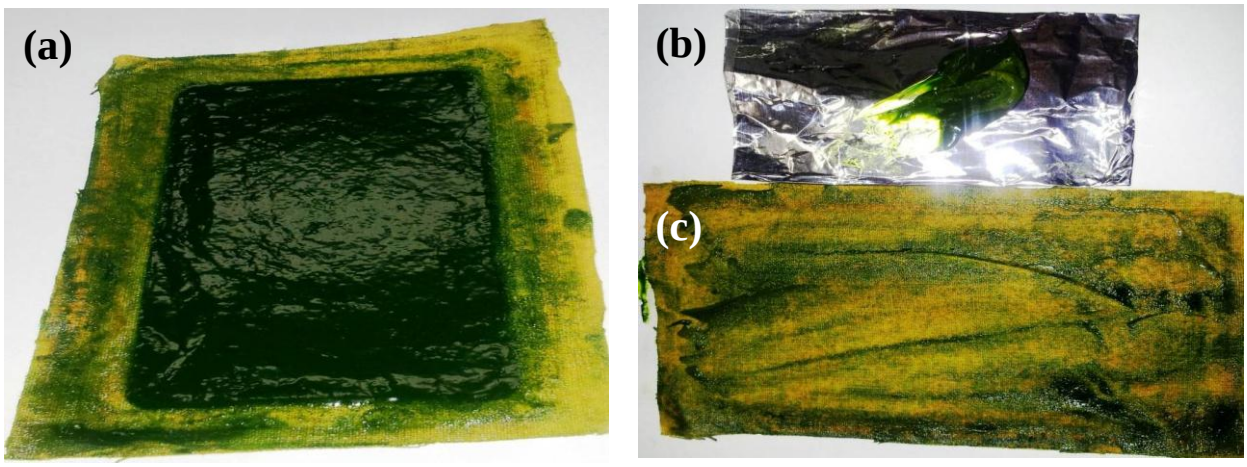

Figure S13. Photographs of the recycled cotton membrane after microalgae harvesting (a) and harvested microalgae biomass (b), and cotton membrane after removing microalgae biomass on the aluminum foil (c). Note that the microalgae harvest was performed three times using the same cotton membrane.